Shoreline Changes and Sediment Transport along Nhat Le Coast, Vietnam

Vu Dinh Cuong
Key Laboratory of River and Coastal Engineering (KLORCE) - Vietnam Academy for Water Resources, Vietnam
cuongvd.vkhtlvn@gmail.com

Nguyen Thanh Hung
Key Laboratory of River and Coastal Engineering (KLORCE) - Vietnam Academy for Water Resources, Vietnam
nthung@vawr.org.vn (corresponding author)

Tran Dinh Hoa
Vietnam Academy for Water Resources, Vietnam
tranhoa08@gmail.com

Nguyen Tien Thanh
Thuyloi University, Vietnam
thanhnt@tlu.edu.vn

Received: 27 December 2023 | Revised: 12 January 2024 | Accepted: 18 January 2024

 DOI: https://doi.org/10.48084/etasr.6822

ABSTRACT

One of the most beautiful beaches in Northern Vietnam, Nhat Le, has recently experienced severe erosion as a result of the ensemble interaction of natural factors, such as tropical cyclones, extreme weather events, and human activities. Consequently, negative impacts on tourism and social and economic development have been recorded. This paper aims to provide a deep understanding of the changes in shoreline and longshore sediment transport at Nhat Le estuary based on two modules of LITDRIFT and LITLINE of the LITPACK software package combined with geospatial analysis. The rate of change statistics is calculated using the Digital Shoreline Analysis System (DSAS) from 30-year multi-temporal satellite data (1989-2019) for multiple historical shoreline positions. The Module of LITDRIFT is employed to estimate sediment transport and the shoreline position calculated from the LITLINE module. These data are then compared with measured topographic data and satellite images. Wave climate conditions are incorporated into the LITDRIFT module to identify the volume of sediment transport along the coast on seasonal and annual bases. The results illustrate that a mean erosion rate of about 2 m per year was observed in the southern sandspit of Nhat Le from 1989 to 2019. This rate reaches 4.5 m per year during 2009-2019.

Keywords-Nhat Le beach; shoreline change; littoral sediment transport; LITPACK model; DSAS

I. INTRODUCTION

Vietnam is one of the countries affected by global climate change, especially in coastal zone and river deltas. With over 3,260 km and about more than 20 million people living on the Vietnamese coastline, it is one of the most densely populated areas in Southeast Asia. Furthermore, Vietnam is experiencing rapid urban and economic growth, and faces a high risk of coastal hazards related to tropical cyclones, floods, or extreme heavy rainfall. Natural coastal erosion may be caused by nearshore currents, wind, waves, weathering, or as a consequence of a reduction in river discharge through decreasing rainfall or snowmelt [1-2]. In other words, accretion could also relate to river discharge during the rainy season or through increasing rainfall and the coasts are likely supplied by river sediment. River discharge and sediments from the river can be controlled by dam systems or weather patterns [3-5]. Many researches state that coastal erosion induced by human is often associated with the construction of river dams, sand mining, and the construction of coastal infrastructure (e.g. groynes, ports, inlet jetties, breakwaters, and sea walls) [6-10]. The important role of non-climatic anthropogenic drivers for the increasing vulnerability of low-lying coastal communities besides long-term and very slow nature impacts of sea level rise is studied in [11]. Accelerated sea level rise could lead to the permanent or frequent inundation of unprotected low-lying land. Combined with climate conditions and storm surge activities, such areas are at a high risk of land subsidence or coastline retreat. All these factors constitute big challenges for understanding the shoreline changes and sediment transport in coastal regions generally and in Vietnam particularly. In the Central coast of Vietnam, more than one fifth of the coastline is being eroded, whereas coastal erosion has become one of the most serious environmental issues in Vietnam, affecting the national economy and social development [12]. For example, severe erosion is observed in Cua Dai beach, Hoi An City [13] and Hai Hau [14-15]. Specifically, Nhat Le and Bao Ninh are long sandy beaches (16 km long) located around Nhat Le estuary, and Nhat Le beach is one of the most beautiful beaches on the North Central coast of Vietnam. In recent years, there has been coastal erosion, particularly in the northern commune of Hai Thanh and the southern commune of Bao Ninh in Nhat Le mouth. The erosion has caused direct damage to coastal houses and infrastructure, and has had a significant impact on coastal tourism. The appearance of a coastal sand dune system is a multifaceted unfavorable topographical factor. For instance, under the influence of the wind, the phenomena of flying and flowing sands have caused sand dunes to gradually move towards the continent, narrowing the already small coastal plain and increasing flooding occurrences, especially in Nhat Le estuary. This may prevent individuals from insightfully understanding the regime of sediment transport, accretion-erosion and shoreline changes in the specific area. Within the coastal zone management, the prediction of coastal evolution with numerical models has proven to be a powerful technique to assist in the comprehension of the processes involved in the performance of necessary interventions and the selection of the most appropriate project design [16]. One-dimensional coastal morphology models (one-line models) have demonstrated practical capability in predicting long-term shoreline change [17]. One-line theory implies that all contour lines have similar shapes and move landward and seaward together up to a limiting offshore depth, the depth of closure, as if there were only one contour line [18]. Thus, one contour line can be used to describe changes in the beach plan shape and volume as the beach erodes and accretes. Many numerical models based on the one-line theory have been implemented for predicting coastal line changes. A well-known numerical model for shoreline change phenomena is LITPACK. Parameters such as wind, wave, current, and water level crucially affect sediment transport phenomena and they should be thus supplied as inputs for the numerical models which are taken from a two-dimensional (2D) hydrodynamics model (MIKE 21FM for this study).

Monitoring coastal areas in developing countries generally and in Vietnam particularly has always been an issue in that it could not provide an accurate identification of the location, the direction, and the geometric shape of the shoreline for a long time period. This information is vital to monitor and model the coastal erosion/accretion processes. To conduct the shoreline monitoring, the traditional methods of ground survey are not only time-consuming, but also not practical enough for large area monitoring. So, the remote sensing analysis method has been deployed in many studies regarding different countries [19-22]. In Vietnam, many researches applied the Digital Shoreline Analysis System (DSAS) to detect the shoreline changes. Based on this technique, authors in [23] employed statistical measures of Net Shoreline Movement (NSM) and End Point Rate (EPR) involved in DSAS for monitoring the shoreline changes in the district of Ky Anh, Ha Tinh province from 1989 to 2013 with only five satellite images. Authors in [24] used DSAS to detect changes in shoreline without estimating the volume of sediment transport for Nhat Le estuary [24]. Utilizing a series of 10 optical satellite images (Landsat and Sentinel-2) from 2010 to 2020 and the statistical models of NSM, EPR, and Linear Regression Rate (LRR) are deployed for 5-year and 50 m intervals. The study pointed out the highest coastal erosion rate for the periods of 2010-2015 and 2015-2020, which is -5.94 m and -2.37 m per year, respectively. Furthermore, the highest accretion rate for these periods was found to be 2.05 m and 3.43 m per year. With four satellite images and DSAS, the shoreline changes for Dong Thap province, Vietnam from 2005 to 2019 were detected [25]. Shoreline changes in other provinces in Vietnam have been estimated using DSAS [26, 27]. Generally, DSAS technique has been widely applied, but its use in combination with LITPACK for understanding the shoreline changes and sediment transport in Nhat Le estuary is limited.

Therefore, the goal of this study is to deeply identify (1) the erosion-accretion evolution along the coast of Nhat Le and (2) the volume and direction of sediment transport along the coast in a seasonal and an annual scale. In order to achieve these targets, the DSAS technique combined with LITPACK software are applied to identify the rate of change and sediment transport for multiple historical coastline positions along the Nhat Le coast. The satellite images of Landsat and Sentinel from 1989 to 2019 were extracted and utilized. The coastal dynamics were digitized, visualized, and compared by two statistical parameters provided in DSAS, namely Shoreline Change Envelope (SCE) and LRR. The Linear Regression (LR) method of determining shoreline position change rate is an important technique, as it minimizes potential random error and short-term variability (cyclical changes) through the use of a statistical approach [28].

II. STUDY AREA

Nhat Le is the estuary of Nhat Le river originating from the Truong Son Cordillera with two major tributaries, Dai Giang and Kien Giang, and discharges into the sea at Dong Hoi city. Located in the tropical monsoon climate regime, the hydrodynamic regime in the estuary of Nhat Le is controlled by factors like waves, currents, tides and the river. Notably, there are two distinguishing seasons, one rainy (from September to March) and one dry (from April to August). Very heavy rains are mainly recorded in September, October, and November. Torrential rains may occur from July to October causing considerable rainfall and river floods due to severe typhoons coming from the Western Pacific basin. The total flows of four months of the flood season (September – December) produce 76% of the annual flow. The tidal regime in the estuary of Nhat Le is mainly characterized by semidiurnal tidal patterns with tidal amplitudes varying averagely from 0.7 to 0.8 m. The maximum and minimum values are over 1.61 m and 0.05 m, respectively [29].

Fig. 1. Sketch map of the study area.

III. MATERIALS AND METHODS

A. Materials

Landsat satellite images from 1989 to 2019 were acquired and freely downloaded from the United States Geological Survey (USGS) web-site (https://earthexplorer.usgs.gov). Images of Landsat satellite and Sentinel-2 images have a spatial resolution of 30 m and 10 m, respectively. Sentinel-2 image snapshotted on November 2nd, 2018 was used to verify the simulations of the changes in the shoreline from the module LITLINE. For the study area, the selected images were downloaded on the basis of several criteria: (1) One image per year and from the dry season (from February to June), (2) cloud cover less than 10% to limit unwanted atmospheric effects, and (3) the images should be at the same sea level (around mean sea level - national datum). A total of 30 images were selected according to these criteria.

B. Detection of Shoreline Changes using DSAS

DSAS is an add-in to Esri ArcGIS (a free available ArcGIS extension) designed by the USGS. It enables a user to detect shoreline movements in tempo-spatial scales and to capture the expansion and regression in coastline morphology. Furthermore, it facilitates calculating rate-of-change statistics from multiple historical shoreline positions. The shoreline is precisely identified through the process of handling remote sensing images, including the following steps:

- Calculating NDWI (Normalized Difference Water Index) to separate a water object from other objects [30].
- Dividing and separating shorelines based on the NDWI index. The DSAS creates straight lines perpendicular to the baseline and inter-sects the shoreline, thereby calculating the variability of shoreline based on the distance from the shoreline point to the baseline.

DSAS provides various methods in defining the rate-of-change statistics (e.g. SCE, EPR, and LRR). For this study, SCE and LLR were selected to calculate the coastline change. SCE is the distance between the shoreline furthest from and closest to the baseline at each transect. It represents the total change in shoreline movement for all shoreline positions [31]. The LRR is calculated using the least square regression lines from all shoreline positions along the transect. The rate of change in shoreline is defined by the slope of the regression line. LRR has typically the advantage of using all the time-series data and discarding the impact of spurious values on the overall accuracy of change rate [32].

C. Modeling of Sediment Transportation

LITPACK model, developed by DHI is a software package for simulating non-cohesive sediment transport in wave and currents, littoral drift, coastline evolution, and profile development along quasi-uniform beaches [33]. The model employs a fully deterministic approach to estimate longshore transport. It consists of the modules of Longshore current and littoral drift (LITDRIFT), coastline evolution (LITLINE), cross-shore profile evolution (LITPROF), and sedimentation in trenches (LITTREN). The applied LITDRIFT and LITLINE modules calculate the amount of sediment transport on the coast and simulate the coastal response to gradients in the alongshore sediment transport under the conditions of waves, water level, and topography. Both models are based on one-line theory in which the cross section of shoreline is assumed to be unchanged during erosion/accretion for shoreline change modeling. It is worth noting that LITLINE calculates the coastline evolution. Then, LITDRIFT module is used for the estimation of longshore Sediment Transport (ST) rates. The module includes important ST mechanisms, such as non-linear wave motion, turbulent bottom boundary layer, wave breaking, and sediment grading. LITDRIFT computes longshore sediment transport from a time series of waves, water level parameters, and cross-shore profile characteristics. Other parameters, like graded sediments, currents, wind, and local roughness can be included as input data.

D. Model Setup and Validation

1) Model Setup

The LITPACK model is setup for two coastline segments around Nhat Le estuary. The first segment is located in the north site of Nhat Le beach with a length of 8 km and the other in the south site of Bao Ninh beach with a length of 6 km. Each segment is divided into 9 cross-sections labeled from CR_L1 to CR_L9 for the north coastline and CR_R1 to CR_R9 for the south coastline. Further divisions are performed between the cross-sections to create 800 and 600 sub-sections with a length of 10 m. Everything is selected as an input for the model. Locations of shoreline and cross-shore profile are displayed in Figure 2. The data used for setting up the models were utilized as follows:

- The cross-shore profiles were extracted from the topographic map from the baseline to the seabed points at elevation of around -12m, producing cross-shore profiles of 1935 m length. This length was set to 5 m resolution to the model with 387 points.
- A sediment characteristics' database on the analysis of the bottom sediment samples collected at the sites entailed in the survey was constructed. Average particle diameter D50 value ranged from 0.3 mm to 0.4 mm, while sediment sorting varies from 1.6 to 2.0. The calculation set the bottom roughness equal to 0.035 uniformly for all sections.
- Wave and water level characteristics at the cross-shore profiles were extracted from the results of Mike21FM

model [34]. Figure 2 shows a wave rose in the offshore and 6 wave roses in the near shore at the study area. The tidal water level in the study ranged from -0.9 m to 0.7 m.

- Shoreline data were extracted from the topographic map and Sentinel images in April 2018 and October 2018

2) Model Validation

There are two steps for validating the LIPPACK model. As the first step, LITDRIFT module is validated with the volume of longshore sediment transport analyzed from topographic data obtained in April 2018 and October 2018 for cross-shore profiles. The sediment volumes in Table I reveal that the calculated sediment volume from LITDRIFT is reasonably consistent with the measured sediment volume from the survey. A difference of less than 40% between the calculated and the measured sediment volume is observed in Table I. In other words, the model can simulate real-world conditions with an accuracy degree of more than 60%. This could be acceptable for sediment transport modeling. Based on this, LITDRIFT module can be used for the calculations of longshore sediment transport.

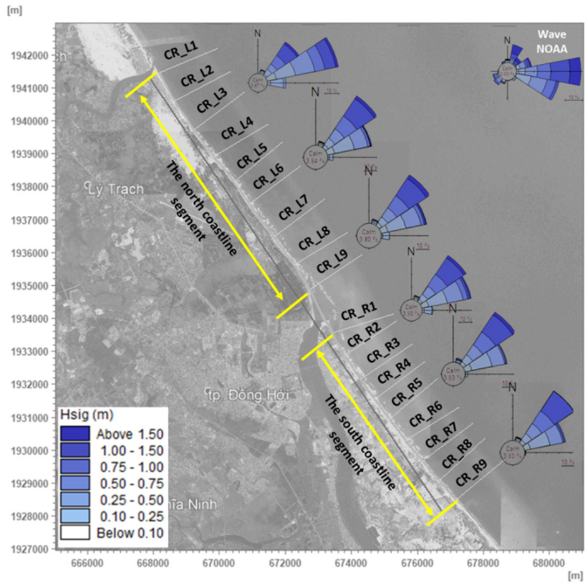

Fig. 2. Sketch map of the study area.

TABLE I. COMPARISON BETWEEN MODELED AND MEASURED SEDIMENT VOLUME (m^3)

Sediment volume from cross-section	CR_L6-CR_L7	CR_L7-CR_L8	CR_L8-CR_L9	CR_R1-CR_R2	CR_R2-CR_R3	CR_R3-CR_R4
Modeled	24.07	28.46	26.23	25.65	18.31	21.22
Measured	38.98	28.54	36.41	30.24	30.54	34.73
Relative error (%)	38.2	0.03	27.9	15.2	39.9	38.9

As the second step, LITLINE module was setup using the cross-shore profiles and sediment characteristics from the first step. The outputs of LITLINE were validated with the shoreline data analyzed from satellite images and topographic data. The shoreline positions calculated using LITLINE module from April 2018 to October 2018 were considered as the initial shoreline position. The calculated shoreline positions were calibrated with the observed shoreline data as the results of field surveys and of the Sentinel image analysis. Figure 3 demonstrates a close correlation between modeled and observed shoreline with a correlation coefficient greater than 0.9. Generally, the modeled shoreline is highly consistent with the measured shoreline for both north and south coast-lines.

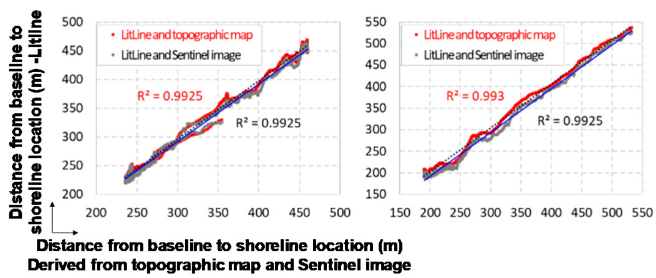

(a) (b)

Fig. 3. Correlation between modeled and observed data. (a) Nortth coastline, (b) south coastline.

IV. RESULTS AND DISCUSSION

A. Shoreline Changes from DSAS Analysis

In this study, the coastline was divided into 160 cross sections with 100 m equidistance from each other, as depicted in Figure 4. It is worth to note that this division is different from the division using the LITPACK model. The time periods are divided into 10-year intervals to detect the rate of shoreline changes. From that, the three periods of 1989-1999, 1999-2009, and 2009-2019 were analyzed within the overall 1989-2019 period. An important point for this selection is that Nhat Le estuary is strongly affected by sediment transporting from the river under the extreme flood events in 1990, 1999, 2009, and 2020.

The indicators of SCE [35] and LRR [36-37] were used to assess the rate of change statistics in the coastline of Nhat Le beach. A typical example of the regression line for 18 transects located in the north coastline is illustrated in Figure 5. The distances from the shoreline points to the baseline are represented by circle points and the dashed line is a linear regression line in the form y = ax + b with coefficient a representing the slope of the line. The accretion rate is described as the shifting of the shoreline towards the seaward side with positive values of LRR, whereas the erosion rate is documented as the shoreline shift landward with the negative values of LRR. Figures 6 and 7 portray a variation in the mean rate of accretion and erosion in the selected four periods in Nhat Le coast using SCE and LRR, respectively. Especially, it is illustrated that during 1989-1999, the sandspit in the south of Nhat Le estuary is strongly eroded with a rate of 3.2 m/year, whereas the sandspit in the north of Nhat Le estuary is strongly accreted with a rate of 4.5 m/year. A mean erosion rate of 3.5 m/year is found in the south coastline at the position of 100 m from the river mouth. During 1999-2009, the mean accretion rate of 3 m/year is smaller than the mean erosion rate in the previous period in the southern sandspit.

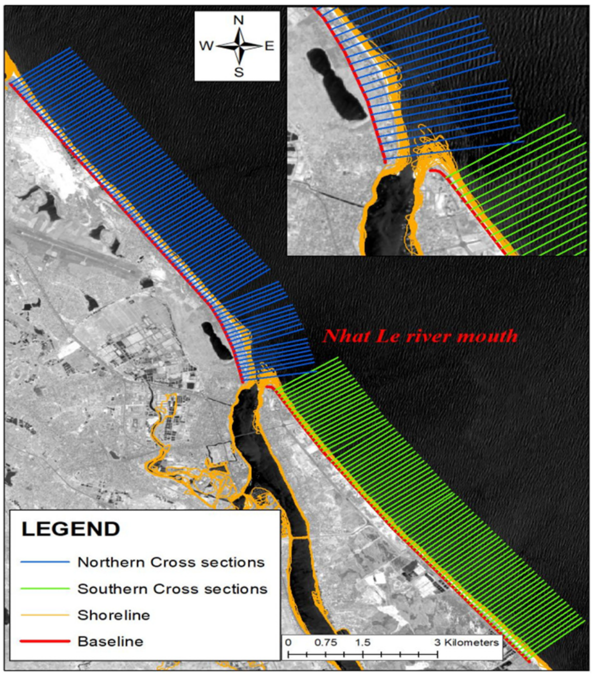

Fig. 4. Position of calculated and observed shorelines.

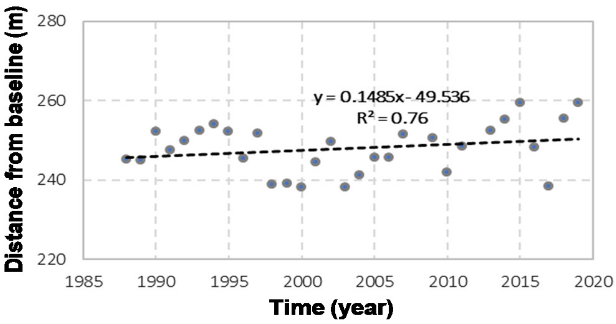

Fig. 5. Linear regression graph at cross section No 18.

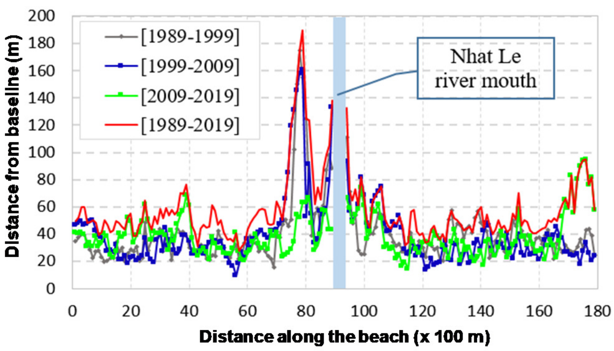

Fig. 6. SCE indicator to evaluate shoreline variability.

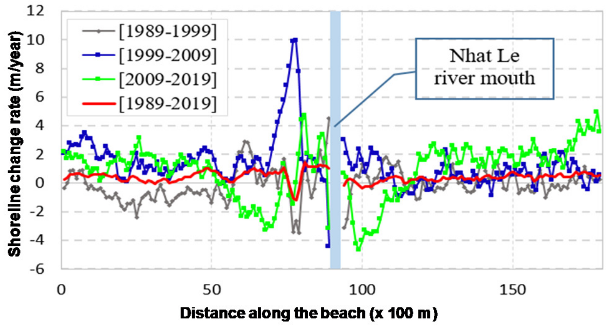

Fig. 7. LRR indicator to evaluate shoreline variability.

The maximum mean accretion rate of 10.1 m/year is discovered at the position of 100 m towards the north side from the river mouth. The sandspit in the north of Nhat Le estuary is the greatest one eroded with a rate of 4.5 m/year. During 2009-2019, there is a strong erosion in the southern sandspit with a rate of 4.5 m/year. Over the entire 1989-2019 period, the mean erosion rate 2 m/year and 1.2 m/year is recorded in the southern sandspit of Nhat Le estuary and at the position of 120 m from the Nhat Le estuary towards north, respectively. Using the SCE and LRR indicators reveals that the most significant shoreline changes are mainly concentrated in the vicinity of Nhat Le river mouth for all the three considered 10-year periods and the entire 1989-2019 period. These changes progressively decrease towards the sides of the mouth. A detailed analysis of shoreline changes, with a particular focus on the area near the Nhat Le estuary is shown in Figure 8. The large change rate of shoreline is definitely related to big sediment movement.

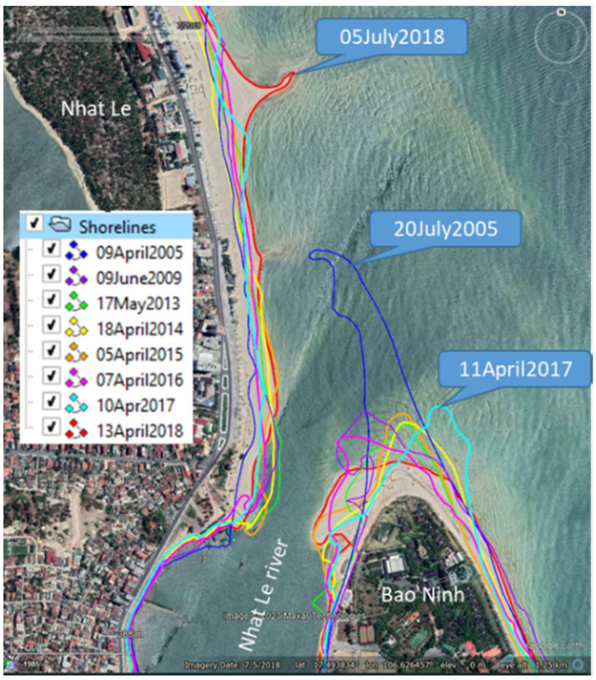

Fig. 8. Shoreline changes along the Nhat Le coast.

B. Longshore Sediment Transport

Obviously, understanding the sediment transport around estuaries and the longshore is crucial in formulating effective solutions to stabilize the shoreline. The longshore sediment transport can be calculated to determine the volume and direction in Nhat Le beach using the modules of the LITPACK model. LITDRIFT is applied in order to estimate the sediment transport along the coast of Nhat Le beach. Furthermore, the wave regime in the sea is calculated for a representative year, considering two distinct seasons, namely the northeast monsoon from October to March and the southeast monsoon from April to September. To measure the long-shore sediment transport, the wave and wind data from the WAVEWATCH III model (point at 17.5^{o}N and 107^{o}E) (http: //www.noaa.gov/) with 2 parameters of direction and magnitude in 2013 are used. The selection of this year is due to the landfall of WUTIP tropical storm and the caused power loss in Quang Binh province. The wave data for boundary conditions of the LITDRIFT module were computed by the Mike21FM model [33]. The sediment transport results for the typical year 2013 calculated from the LITDRIFT module are depicted in Figure 9 and Table II.

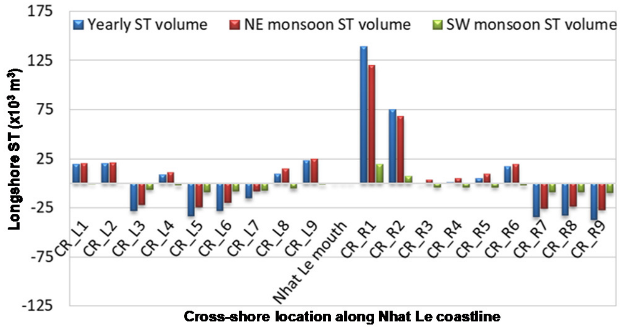

Fig. 9. Volumes of longshore sediment transport in annual and seasonal scales.

TABLE II. VOLUMES OF SEDIMENT TRANSPORT AT CROSS SECTIONS IN AN ANNUAL AND SEASONAL SCALE OF NORTHWEST AND SOUTHEAST MONSOON

Cross sections	Annual (× 10^3 m^3/year)		Northeast monsoon (× 10^3 m^3/year)		Southwest monsoon (× 10^3 m^3/year)	
	Net sediment transport from north to south	Total sediment transport	Net sediment transport from north to south	Total sediment transport	Net sediment transport from north to south	Total sediment transport
CR_L1	19.45	49.9	20.4	36.47	-0.94	13.43
CR_L2	20.41	47.26	20.87	34.73	-0.46	12.53
CR_L3	-28.26	42.77	-21.9	32.14	-6.36	10.63
CR_L4	8.73	44.2	10.94	31.58	-2.21	12.62
CR_L5	-33.29	55.15	-24.12	39.87	-9.17	15.28
CR_L6	-27.99	54.96	-19.97	40.04	-8.02	14.92
CR_L7	-15.12	55.66	-7.81	39.17	-7.31	16.49
CR_L8	9.2	76.37	14.39	54.67	-5.19	21.7
CR_L9	22.81	59.35	24.33	43.33	-1.52	16.02
Nhat Le river mouth						
CR_R1	139.1	149	120	122.9	19.1	26.1
CR_R2	75.1	98.57	68.03	77.55	7.07	21.02
CR_R3	-0.45	47.36	3.57	33.97	-4.02	13.39
CR_R4	0.79	45.04	4.85	31.85	-4.06	13.19
CR_R5	4.84	52.49	9.06	37.06	-4.23	15.43
CR_R6	16.72	59.67	19.09	42.89	-2.37	16.78
CR_R7	-34.43	52.98	-25.48	38.88	-8.95	14.1
CR_R8	-32.73	50.8	-23.69	36.69	-9.04	14.11
CR_R9	-36.91	53.18	-27.13	38.78	-9.78	14.4

As displayed in Figure 9, volumes of longshore sediment transport for 18 cross-shore profiles along the Nhat Le coastline are exposed to the annual and seasonal scales of northeast and southwest monsoons. Generally, the volume of sediment transport during the northeast monsoon is greater than that during the southwest monsoon. There is a shift from the south towards the north during the southwest monsoon. For cross sections CR_L1, CR_L2, CR_L4, and CR_L8 to CR_L9 in the north coastline of Nhat Le river mouth, the movement of net sediment transport is from the north to the south with the approximate volume of 20 × 10^3 m^3/year. On the contrary, the movement of net sediment transport from the south to the north with the volume of over 20 × 10^3 m^3/year is observed for the other cross sections (CR_L3, CR_L5 to CR_L7). It is worth noting that the largest volume of sediment transport with over 70 × 10^3 m^3/year is observed in cross sections CR_R1 and CR_R2, located near the river mouth. This volume is shifted from the north towards the south. There is a similar movement at the cross sections CR_R3 to CR_R6, but the volumes of sediment transport remarkably decrease by under 15 × 10^3 m^3/year). The volume of sediment transport at the cross sections CR_R7 to CR_R9 is notably increased again by over 20 × 10^3 m^3/year from south to north. This reveals that sediment transport volumes substantially fluctuate in spatial-temporal scale.

Table II displays the volumes of net and total sediment transport at all cross sections. The negative values indicate the direction of sediment transport from south to north. In an annual scale, sediment transport volume of cross sections is mostly estimated from 40 to 60 strongly 10^3 m^3/year. This value is higher at several cross sections, e.g. CR_L8 (76 × 10^3

m^3/year), CR_R2 (98 × 10^3 m^3/year), and CR_R1 (149 × 10^3 m^3/year). Among that, total sediment transport volume of roughly 30 to over 40 × 10^3 m^3 at these cross sections is observed during the northeast monsoon season. A larger amount of sediment transport is found out at cross sections CR_L8 (over 54 × 10^3 m^3), CR_R2 (77 × 10^3 m^3), and CR_R1 (122 × 10^3 m^3). Notably, the volume of sediment transport at the cross sections is smaller with values from over 10 to under 17 × 10^3 m^3. Some cross sections have larger volumes, such as CR_L8, CR_R2, and CR_R1 with over 21 × 10^3 m^3, 21 × 10^3 m^3, and 26 x 10^3 m^3, respectively. There are large volumes of sediment transport at the CR_L4, CR_L8, and CR_R3 to CR_R5 cross sections but small net sediment transport. There is a similarity in the volume of sediment transport at these cross sections from north to south and south to north.

Figure 10 illustrates the results in the volume of sediment transport with its distribution at four typical cross sections along the coastline located in the north and south of Nhat Le estuary. CR_L6 and CR_L9 represent the north whereas CR_R6 and CR_R1 represent the south of Nhat Le estuary. Cross sections CR_L6 and CR_R6 are significantly far from the estuary, whereas the others are close. It can be observed that for the cross-sections along the straight coast, far from the river mouth, the morphology of the slope cross-section is relatively uniform. The distribution of sediment transport quantity along the shore is concentrated in a relatively narrow beach cross-section, approximately 300-400 m wide, coinciding with the coastal wave breaking zone. This distribution follows a curve with a single peak, as depicted in Figures 10(a) and 10(c). At cross section CR_L6, the total sediment transport (Net drift) is from the south to the north. So, the dominant sediment transport component is from the south to the north (Drift -ve), while the sediment transport component from the north to the south (Drift +ve) is less significant. The largest total amount of sand and mud transport reached 425 m^3/s/m. At cross section CR_R6, the total sediment transport volume is from the north to the south, because the dominant sediment transport component is from the north to the south, surpassing the sediment transport component from the south to the north. The largest total amount of sediment transport reached 175 m^3/s/m. Therefore, the total amount of sediment transport at section CR_L6 on the north coast and at section CR_R6 on the south coast is relatively small and shows minimal variation.

Furthermore, for the coast near the river mouth, the beach profile exhibits a gentle and irregular shape, characterized by the presence of a raised terrain area known as the shoal bar that obstructs the river mouth. The distribution of sediment transport along the coastline, across the beach cross-section, is considerably broader, spanning a width of approximately 200 m^3/s/m. This distribution takes the form of a curved pattern with two peaks, which is the result of repeated wave breaking occurrences (as depicted in Figures 10(b) and 10(d)). At cross section CR_L9, the total volume of sediment transport is from the north to the south, with the maximum amount reaching 145 m^3/s/m. Conversely, at section CR_R1, the total volume of sediment transport is also from the north to the south, with the largest quantity of sand and mud reaching 1130 m^3/s/m. Consequently, the total amount of sediment transport at cross section CR_R1, located near the river mouth on the south bank, is considerably greater than that at cross section CR_L9, situated near the river mouth on the north bank.

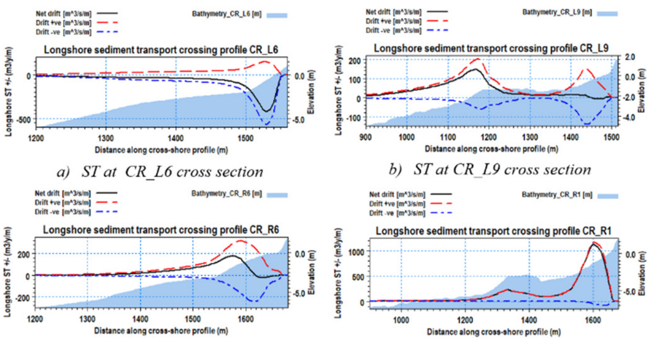

a) ST at CR_L6 cross section *b) ST at CR_L9 cross section*

c) ST at CR_R6 cross section *d) ST at CR_R1 cross section*

Fig. 10. Ranges of sediment transport across cross sections.

V. CONCLUSIONS

The Nhat Le coastline experienced significant changes over a 30-year period from 1989 to 2019, as observed through the analysis of multi-temporal remote sensing images. The coastline variability is particularly pronounced in the vicinity of the Nhat Le river mouth, gradually stabilizing as one moves further away from the mouth. The period from 2009 to 2019 witnessed more substantial shoreline changes compared to the other two periods. More specifically, the shoreline at Hai Thanh commune (located north of the river mouth) and Bao Ninh commune (located south of the river mouth) exhibited an average erosion rate of approximately 5 m per year. These areas experienced ongoing coastal erosion, resulting in the retreat of the shoreline over time.

The direction and volume of longshore sediment transport in Nhat Le beach were calculated with the help of the LITPACK software. The sediment transport exhibits significant variability among different cross-shore sections and between the two monsoon seasons. On average, the total volume of sediment transport through all cross-shore profiles is approximately 50 × 10^3 m^3 per year. However, the highest volume of sediment transport occurs at the southern cross-shore profile close to the river mouth, reaching a value of 122 × 10^3 m^3 per year. This indicates that the sediment transport is influenced by local factors such as the proximity to the river mouth, which can result in higher sediment transport rates in that specific area. The width of cross-shore sediment transport is around within 350 - 400 m along the coast and can be extended to 500 - 600 m for areas near the river mouth

ACKNOWLEDGMENT

This paper was supported by the research projects: KC08.16/16-20 "Research on erosion and accretion along the coast and estuaries from Quang Binh to Thua Thien Hue provinces, considering impacts of the upper reservoirs and proposing solutions" and "Research and propose solutions to stabilize estuaries in the central coastal area for socio-economic development and disaster prevention and pilot application for Thuan An estuary, Thua Thien Hue province".

REFERENCES

[1] E. C. F. Bird, *Coastal Geomorphology: An Introduction*, 2nd ed. Hoboken, NJ, USA: Wiley, 2008.

[2] B.-L. Cui and X.-Y. Li, "Coastline change of the Yellow River estuary and its response to the sediment and runoff (1976–2005)," *Geomorphology*, vol. 127, no. 1, pp. 32–40, Apr. 2011, https://doi.org/10.1016/j.geomorph.2010.12.001.

[3] A. Liaghat, A. Adib, and H. R. Gafouri, "Evaluating the Effects of Dam Construction on the Morphological Changes of Downstream Meandering Rivers (Case Study: Karkheh River)," *Engineering, Technology & Applied Science Research*, vol. 7, no. 2, pp. 1515–1522, Apr. 2017, https://doi.org/10.48084/etasr.969.

[4] D. D. Cham, N. T. Son, N. Q. Minh, N. T. Hung, and N. T. Thanh, "Hydrodynamic Condition Modeling along the North-Central Coast of Vietnam," *Engineering, Technology & Applied Science Research*, vol. 10, no. 3, pp. 5648–5654, Jun. 2020, https://doi.org/10.48084/etasr.3506.

[5] A. N. Laghari, W. Rauch, and M. A. Soomro, "A Hydrological Response Analysis Considering Climatic Variability: Case Study of Hunza Catchment," *Engineering, Technology & Applied Science Research*, vol. 8, no. 3, pp. 2981–2984, Jun. 2018, https://doi.org/10.48084/etasr.2056.

[6] N. T. Hung, D. M. Duc, D. T. Quynh, and V. D. Cuong, "Nearshore Topographical Changes and Coastal Stability in Nam Dinh Province, Vietnam," *Journal of Marine Science and Engineering*, vol. 8, no. 10, Oct. 2020, Art. no. 755, https://doi.org/10.3390/jmse8100755.

[7] J. A. Warrick, A. W. Stevens, I. M. Miller, S. R. Harrison, A. C. Ritchie, and G. Gelfenbaum, "World's largest dam removal reverses coastal erosion," *Scientific Reports*, vol. 9, no. 1, Sep. 2019, Art. no. 13968, https://doi.org/10.1038/s41598-019-50387-7.

[8] J.-P. Bravard, M. Goichot, and S. Gaillot, "Geography of Sand and Gravel Mining in the Lower Mekong River," *EchoGeo*, no. 26, Dec. 2013, Art. no. 13659, https://doi.org/10.4000/echogeo.13659.

[9] C. Jordan *et al.*, "Sand mining in the Mekong Delta revisited - current scales of local sediment deficits," *Scientific Reports*, vol. 9, no. 1, Nov. 2019, Art. no. 17823, https://doi.org/10.1038/s41598-019-53804-z.

[10] K. F. Nordstrom, "Living with shore protection structures: A review," *Estuarine, Coastal and Shelf Science*, vol. 150, pp. 11–23, Oct. 2014, https://doi.org/10.1016/j.ecss.2013.11.003.

[11] "Special Report on the Ocean and Cryosphere in a Changing Climate," *IPCC*. https://www.ipcc.ch/srocc/.

[12] H. N. Thanh, *National Research project coded KC08.16/16-20. Research on erosion and accretion along the coast and estuaries from Quang Binh to Thua Thien Hue provinces, considering impacts of the reservoirs and proposing solutions.* Hanoi, Vietnam: Key Laboratory of River and Coastal Engineering, 2019.

[13] D. D. Cham, N. Q. Minh, N. T. Lam, N. T. Son, and N. T. Thanh, "Identification of Erosion-Accretion Causes and Regimes Along the Quang Nam Coast, Vietnam," in *10th International Conference on Asian and Pacific Coasts*, Hanoi, Vietnam, Sep. 2019, pp. 809–814, https://doi.org/10.1007/978-981-15-0291-0_111.

[14] D. M. Duc, K. Yasuhara, N. M. Hieu, and N. C. Lan, "Climate change impacts on a large-scale erosion coast of Hai Hau district, Vietnam and the adaptation," *Journal of Coastal Conservation*, vol. 21, no. 1, pp. 47–62, Feb. 2017, https://doi.org/10.1007/s11852-016-0471-7.

[15] N. T. Thanh and N. H. Son, "Understanding Shoreline and Riverbank Changes Under the Effect of Meteorological Forcings," in *10th International Conference on Asian and Pacific Coasts*, Hanoi, Vietnam, Sep. 2019, pp. 1303–1310, https://doi.org/10.1007/978-981-15-0291-0_177.

[16] H. Hanson *et al.*, "Modelling of coastal evolution on yearly to decadal time scales," *Journal of Coastal Research*, vol. 19, no. 4, pp. 790–811, 2003.

[17] M. Dabees and J. W. Kamphuis, "Oneline, A Numerical Model for Shoreline Change," pp. 2668–2681, Dec. 2015, https://doi.org/10.1061/9780784404119.202.

[18] J. W. Kamphuis, *Introduction To Coastal Engineering And Management*, 3rd ed. Hackensack, NJ, USA: World Scientific, 2020.

[19] Y. Song, Y. Shen, R. Xie, and J. Li, "A DSAS-based study of central shoreline change in Jiangsu over 45 years," *Anthropocene Coasts*, vol. 4, no. 1, pp. 115–128, Jan. 2021, https://doi.org/10.1139/anc-2020-0001.

[20] R. M. Abou Samra and R. R. Ali, "Applying DSAS tool to detect coastal changes along Nile Delta, Egypt," *The Egyptian Journal of Remote Sensing and Space Science*, vol. 24, no. 3, Part 1, pp. 463–470, Dec. 2021, https://doi.org/10.1016/j.ejrs.2020.11.002.

[21] K. Nassar, W. E. Mahmod, H. Fath, A. Masria, K. Nadaoka, and A. Negm, "Shoreline change detection using DSAS technique: Case of North Sinai coast, Egypt," *Marine Georesources & Geotechnology*, vol. 37, no. 1, pp. 81–95, Jan. 2019, https://doi.org/10.1080/1064119X.2018.1448912.

[22] M. M. Billah, "Mapping and Monitoring Erosion-Accretion in an Alluvial River Using Satellite Imagery – The River Bank Changes of the Padma River in Bangladesh," *Quaestiones Geographicae*, vol. 37, no. 3, pp. 87–95, Sep. 2018, https://doi.org/10.2478/quageo-2018-0027.

[23] T. N. An, "An application of digital shoreline analysis system (dsas) to study shoreline change along ky anh coasts (ha tinh province) during 1989-2013," *Science Journal of Natural Resources and Environment*, vol. 21, pp. 66–72, Jun. 2019.

[24] H. Le, N. Quang, V. Tuan, and M. H. Nguyen, "Analyzing River Estuary Changes Using Remote Sensing Images, a Case Study of Nhat Le River of Quang Binh Province," *TNU Journal of Science and Technology*, vol. 227, no. 3, pp. 15–24, Feb. 2022, https://doi.org/10.34238/tnu-jst.5409.

[25] T. T. Kim, P. T. M. Diem, N. N. Trinh, N. K. Phung, and N. T. Bay, "Riverbank movement of the Mekong River in An Giang and Dong Thap Provinces, Vietnam in the period of 2005–2019," *Vietnam Journal of Hydrometeorology*, vol. 6, pp. 35–45, 2020.

[26] D. V. To and P. T. P. Thao, "A shoreline analysis using DSAS in Nam Dinh coastal area," *International Journal of Geoinformatics*, vol. 4, no. 1, pp. 37–42, Mar. 2008.

[27] H.-H. Nguyen, C. McAlpine, D. Pullar, S. J. Leisz, and G. Galina, "Drivers of Coastal Shoreline Change: Case Study of Hon Dat Coast, Kien Giang, Vietnam," *Environmental Management*, vol. 55, no. 5, pp. 1093–1108, May 2015, https://doi.org/10.1007/s00267-015-0455-7.

[28] B. C. Douglas and M. Crowell, "Long-Term Shoreline Position Prediction and Error Propagation," *Journal of Coastal Research*, vol. 16, no. 1, pp. 145–152, 2000.

[29] N. Dai, *Collection and adjustment of meteorological and hydrological data of Quang Binh province from 1956 to 2005. Research report.* Department of Natural Resources and Environment of Quang Binh Province, 2006.

[30] S. K. McFEETERS, "The use of the Normalized Difference Water Index (NDWI) in the delineation of open water features," *International Journal of Remote Sensing*, vol. 17, no. 7, pp. 1425–1432, May 1996, https://doi.org/10.1080/01431169608948714.

[31] E. A. Himmelstoss, "DSAS 4.0 Installation Instructions and User Guide," in *Digital Shoreline Analysis System (DSAS) version 4.0 — An ArcGIS extension for calculating shoreline change: U.S. Geological Survey Open-File Report 2008-1278.*, E. R. Thieler, E. A. Himmelstoss, J. L. Zichichi, and A. Ergul, Eds. 2009.

[32] M. G. Honeycutt, M. Crowell, and B. C. Douglas, "Shoreline-Position Forecasting: Impact of Storms, Rate-Calculation Methodologies, and Temporal Scales," *Journal of Coastal Research*, vol. 17, no. 3, pp. 721–730, 2001.

[33] *An integrated modeling system for littoral processes and coastline kinetics, short introduction and tutorial.* Copenhagen, Denmark: DHI, 2009.

[34] N. T. Hung, V. D. Cuong, N. V. Hung, and N. Q. Minh, "Research on Seasonal Variability of Hydrody-Namic Regime in Nhat Le Estuary Area, Quang Binh Province.," *Journal on Science and Technology of Irrigation (Vietnam Academy for Water Resources)*, no. 48, pp. 91–104, Oct. 2018.

[35] E. R. Thieler, D. Martin, and A. Ergul, *The Digital Shoreline Analysis System, version 2.0: Shoreline change measurement software extension for ArcView. USGS Open-File Report 03-076*. USGS, 2003.

[36] E. R. Thieler, E. A. Himmelstoss, J. L. Zichichi, and A. Ergul, "The Digital Shoreline Analysis System (DSAS) Version 4.0 - An ArcGIS

extension for calculating shoreline change," U.S. Geological Survey, Reston, VA, USA, 2008–1278, 2009, https://doi.org/10.3133/ofr20081278.

[37] W. A. Ali, M. F. Kaiser, S. Kholief, and M. El-Tahan, "Assessment of coastal changes along Baltim resort (Egypt) using remote sensing and DSAS method," *Egyptian Journal of Aquatic Biology and Fisheries*, vol. 21, no. 1, pp. 37–48, May 2017, https://doi.org/10.21608/ejabf.2017.2380.